Environ. Sci. Technol. **2005**, *39,* 6052−6062

Carbon Isotope Fractionation of Organic Contaminants Due to Retardation on Humic Substances: Implications for Natural Attenuation Studies in Aquifers

FRANK-DIETER KOPINKE,*
ANETT GEORGI,
MICHAEL VOSKAMP, AND
HANS H. RICHNOW

Departments of Environmental Technology and Isotope Biogeochemistry, UFZ Centre for Environmental Research Leipzig-Halle Ltd., Permoserstrasse 15, 04318 Leipzig, Germany

Experimental approaches were developed which permit the measurement of carbon isotope effects during partitioning of organic compounds between water and humic substances. Fractionation factors $\alpha_{sorption} = K_{OC}^{12C}/K_{OC}^{13C}$ for carbon isotopomers of benzene (1.00044 ± 0.00015) and toluene (1.00060 ± 0.00010) were determined from a 10-step batch experiment. Similar fractionation factors were estimated for benzene (1.00017), 2,4-dimethylphenol (1.00035), and *o*-xylene (≤1.00092) from chromatographic experiments. The latter method is based on chromatographic amplification of the fractionation effect ($\Delta\delta^{13}C$) in an HPLC column with humic acid (HA) as the stationary phase. Possible implications of the sorption-based isotope fractionation for assessment of natural attenuation processes in contaminated aquifers are discussed. Depending on the aquifer properties (organic carbon content, heterogeneity) together with the plume source, length, and status (stationary or expanding), scenarios may be constructed where sorption-based isotope fractionation competes significantly with that caused by chemical or microbial degradation processes.

Introduction

A major challenge in contaminant hydrology is to determine the fate of organic contaminants in aquifers. Reliable methods for the assessment of in situ biodegradation are required in the context of natural attenuation approaches. Isotope fractionation of organic contaminants during biodegradation is held to be a useful tool for tracing the in situ biodegradation in contaminated aquifers (*1*−*3*). Recently, concepts have been developed to estimate the extent of in situ biodegradation using compound-specific isotope fractionation factors and the isotope signatures of contaminants downgradient from a pollution source (*4*, *5*). This concept relies on the presumption that only degradation significantly alters the isotope composition of contaminants in the aquifer. Other processes such as dilution, evaporation, and sorption−desorption which are also involved in the attenuation of contaminants are considered not to affect their isotope composition to a significant extent.

* Corresponding author tel: ++49-(0)341-235-3264; fax: ++49-(0)341-235-2942; e-mail: frank-dieter.kopinke@ufz.de.

Dilution will certainly not affect the isotope composition of dissolved organic contaminants. The geological situation dictates that evaporation of contaminants from the groundwater into the unsaturated zone of the soil is unlikely to significantly reduce the mass of contaminants within aquifers. Sorption processes may retard hydrophobic contaminants in the aquifer, controlling at least partly their spatial and temporal distribution in the aquifer. One of the dominant sorption mechanisms is the partitioning of dissolved organic contaminants between groundwater (the mobile phase) and soil or sediment organic matter (SOM, the stationary phase). Moreover, sorption can be an important factor affecting the bioavailability of contaminants for the indigenous microbial communities (*6*).

Little is known about isotope effects during sorption and desorption of contaminants and their influences on the isotope pattern of contaminants in aquifers. Some authors have suggested that hydrophobic sorption may not affect the isotope composition of contaminants significantly, and that isotope effects caused by sorption in subsurface systems can thus be neglected (*7*−*9*). However, reversed-phase (RP) chromatography experiments provide clear evidence that sorption can affect the carbon isotope composition of organic substances (*10*, *11*). Commonly, under RP conditions (i.e., the mobile phase is more polar than the stationary phase) the migration of the heavier isotopomers is faster than that of the lighter isotopomers.

It may be implied that, during plume migration the contaminant will undergo a number of consecutive sorption and desorption steps between the mobile water phase and the stationary SOM phase, similar to those known from RP chromatography experiments. To predict the isotope fractionation of hydrophobic sorption in aquifers during migration processes, the cumulative effect of many partitioning steps must be taken into account. To the best of our knowledge, this has not yet been undertaken.

In a first approach, a multistep batch experiment with static sorption equilibria was conducted. In contrast to single-step experiments described in the literature (*8*, *9*), it proved significant carbon isotope fractionation for benzene and toluene. We then performed a number of chromatographic experiments using a silica column coated with humic acid (HA) to simulate dynamic transport processes. These experiments made carbon isotope fractionation clearly observable. On the basis of their results, we developed a model to calculate isotope effects on sorption coefficients $\alpha_{sorption} = K_{OC}^{12C}/K_{OC}^{13C}$, which were derived from chromatographic experiments with benzene, 2,4-dimethylphenol, and *o*-xylene. Finally, we discuss the environmental significance of our findings in the context of boundary conditions for applying the isotope composition of contaminants as an indicator for in situ biodegradation.

Experimental Section

Chemicals. Unless otherwise stated, all chemicals and organic solvents were obtained in reagent quality from Merck (Germany).

GC−MS Measurements. The concentrations of the analytes were determined with a GC−MS (QP-5000, Shimadzu, Japan) operated in single-ion mode.

GC−C−IRM−MS Measurements. The carbon isotope composition of analytes was measured with a GC−C−IRM−MS (gas chromatography−combustion−isotope-ratio-monitoring−mass spectrometry) system, containing a 6890 Series GC system (Agilent Technology, Palo Alto, CA). Aliquots (0.5−5 μL) of extracts were injected in the split mode (1:5)

10.1021/es040096n CCC: $30.25
© 2005 American Chemical Society
Published on Web 07/06/2005

and separated on a capillary column (RTX-5, 60 m × 0.32 mm i.d., 0.5 μm f.t., J&W Scientific, Folsom, CA). The injector temperature was set at 250 °C. The following GC temperature programs were applied: for benzene, 40 °C (4 min), 4 K min^{-1}, 85 °C, 20 K min^{-1}, 150 °C; for 2,4-dimethylphenol, 85 °C (12 min), 8 K min^{-1}, 190 °C; and for *o*-xylene, 60 °C (4 min), 4 K min^{-1}, 105 °C, 20 K min^{-1}, 150 °C. Samples from the batch experiments were analyzed by manual headspace sampling (100−1000 μL, split ratio 1:5 to 1:50, GC temperature program as described above for benzene).

The GC unit was connected to a combustion device (Finnigan MAT GC-III, ThermoFinnigan, Germany) with a modified water removal assembly (Nafion membrane, 50-cm long, $T = 0$ °C) coupled via open split to an isotope-ratio mass spectrometer (Finnigan MAT 252, ThermoFinnigan, Germany). Organic substances in the GC effluent stream were oxidized to CO_2 in the combustion interface held at 940 or 980 °C on a CuO/Ni/Pt catalyst. CO_2 was transferred on-line to the mass spectrometer to determine $^{13}CO_2/^{12}CO_2$ ratios. The instrument was calibrated using a reference gas (CO_2) with known isotope composition, which was calibrated vs IAEA reference materials (*12*) by elemental analysis. All samples were measured in at least 5 replicates. The standard deviation of the single measurements $\sigma(x)$ of the $\delta^{13}C$ values was always better than ± 0.6‰ (δ-notation according to eq 3).

Batch Experiments. Deionized water (1100 mL) was spiked with a methanolic stock solution of methyl-*tert*-butyl ether (MTBE), benzene, and toluene yielding final concentrations of 100, 1000, and 200 ppm, respectively, in the aqueous solution. This solution was agitated with a magnetic stirrer in a 1200-mL glass bottle equipped with a pH electrode and a Mininert valve for headspace sampling. The activity of the dissolved hydrocarbons was measured by GC analysis of headspace samples (25 μL) after establishing the water−headspace equilibrium (≥30 min). Sodium humate (20 g, Sigma-Aldrich Chemie GmbH, Steinheim, Germany, 38 wt % organic carbon) was added. After complete dissolution of the solid material, the pH value was adjusted to about 1.6 by injection of HCl, giving rise to flocculation of the HA. After 1 h the headspace over the HA suspension was analyzed again. The decrease in the headspace concentrations of the analytes was assigned to the sorbed fractions. An extension of the sorption period up to 24 h did not result in significantly higher degrees of sorption. Thus, sorption equilibrium was established within about 1 h. The separation of the HA was carried out by centrifugation (5 min at 10 000 rpm). The clear aqueous solution (residual HA content about 200 mg L^{-1}) was decanted, topped-up by the amount of water lost (50−100 mL in the wet HA flocculate), and used for the next sorption step. In the course of this procedure, the salinity of the solution increased steadily up to about 0.4 M NaCl after 10 sorption steps.

The same procedure was also performed without adding HA. In this control experiment, the depletion of analytes (due to sorption in the HA series) was simulated by replacement of 300 mL of the aqueous solution by pure water. In addition to the concentrations, the isotope composition of the analytes was measured after the 4th and the 10th sorption steps by GC−C−IRM−MS using 1-mL samples from the headspace (5 parallel measurements each). Although headspace sampling may in principle affect the isotope composition of an analyte, this effect is canceled-out in the applied calculations, because HA suspensions and water samples were analyzed by the same procedures and only relative isotope ratios are handled. Moreover, Slater et al. (*13*) found evidence that the fractionation effect is very small for the partitioning of hydrophobic compounds between aqueous solution and the gas phase. The values for the isotope composition are the average of the results of two parallel experiments.

Preparation of the Humic-Acid-Coated HPLC Phase. The HA-coated stationary phase was prepared by a procedure slightly modified from that described in ref *14*. Briefly, 10 g of silica gel with a particle size of 10 μm (Nucleosil 50-10, Macherey-Nagel, Germany) was thoroughly washed with $NH_4OH-H_2O_2-H_2O$ and $HCl-H_2O_2-H_2O$ solutions (both 1:1:5; v:v:v) and then dried at 120 °C under reduced pressure. For preactivation, the dry silica gel was suspended in 170 mL of toluene solution containing 3% of (3-aminopropyl)-dimethyl-ethoxysilane for 1 h, filtered, and dried at 160 °C under reduced pressure for 6 h to remove the excess of (3-aminopropyl)dimethyl-ethoxysilane. A 1.7-g aliquot of HA (Roth, Germany) was dissolved in 150 mL of diluted NaOH at pH 10 and mixed with the pretreated silica gel for 2 h to allow the reaction between the carboxylic groups of the HA and the amino groups of the pretreated silica particles to take place. The solution was then removed by centrifugation. The resulting pellet was repeatedly washed with water until the supernatant was colorless. To obtain an end-capping of the remaining free amino groups, the HA-loaded silica gel was suspended in 50 mL of a solution containing 840 mg of sodium acetate and 330 mg of *N*-(3-dimethylaminopropyl)-*N*′-ethylcarbodiimid hydrochloride (EDC), adjusted to pH 10, and shaken for 4 h. The solution was removed by centrifugation and the resulting precipitate was again suspended in 50 mL of the sodium acetate−EDC−solution and shaken for 4 h, after which the solution was removed by filtration and the filter cake was washed with deionized water until the supernatant became nearly colorless. The HA-loaded silica gel pellet was then freeze-dried. The gel was packed in methanol at 35 MPa into a 250 mm × 4.6 mm HPLC column.

Chromatographic Experiments. Aliquots of 25−50 μL of analyte stock solutions (1 g L^{-1} benzene and 2,4-dimethylphenol, 0.15 g L^{-1} *o*-xylene, respectively) were injected into an HPLC system (1100 HPLC System, Hewlett-Packard, Germany) consisting of a pump, an injection loop, a 250 mm × 4.6 mm HPLC column filled with the HA-coated material described above, and a UV-detector operating at $\lambda = 205$ nm. The HPLC system was operated under isocratic conditions using 10 mM NaCl solution adjusted to pH 5 with HCl as the eluent (1 mL min^{-1}). The pore volume of the column and the break-through curve were determined with KNO_3 as a conservative tracer.

The eluting analyte peaks were separated into 20−40 fractions. Each fraction of benzene and *o*-xylene was extracted from the eluent with 100 μL of *n*-pentane using toluene as internal standard. 2,4-Dimethylphenol was extracted with 100 μL of benzene using *o*-xylene as internal standard. Concentrations and carbon isotope ratios were determined by GC−MS and GC−C−IRM−MS measurements.

Results and Discussion

Batch Experiments. Partitioning of analytes between water and dissolved or suspended organic matter is usually described by means of their sorption coefficients (K_{OC}) as follows:

$$K_{OC} = \frac{C_{\text{analyte sorbed}}}{C_{\text{analyte freely dissolved}}} = \frac{1 - X_{\text{freely dissolved}}}{X_{\text{freely dissolved}}} \cdot \frac{1}{C_{OC}} [\text{L kg}^{-1}] \quad (1)$$

where $X_{\text{freely dissolved}}$ is the freely dissolved analyte fraction ($X_{\text{freely dissolved}} + X_{\text{sorbed}} = 1$) and C_{OC} is the concentration of organic carbon (OC) in the sample. K_{OC} values can be defined for any distinct species including isotopomers of an organic compound. Theoretically, various isotopomers having different numbers and positions of ^{13}C-atoms within the molecule must be considered. For simplification, it was assumed that for low-molecular-weight compounds only two isotopically distinct species must be considered: one ^{12}C-

TABLE 1. Carbon Isotope Composition of the Freely Dissolved Fractions and Sorption Coefficients of Benzene and Toluene in a Multistep Batch Experiment with Suspended Humic Acid (C_{OC} = 7.6 g L^{-1}, pH 1.6)

substance	log K_{OW}	$\delta^{13}C$ [‰] initial solution without HA	blank solution after 10 simulation steps without HA	freely dissolved fraction after *m* sorption steps with HA	$X_{freely\ dissolved}$	$\Delta\delta^{13}C$ [‰]	logK_{OC} (eq 1)	$\alpha_{sorption}$ (eq 4)
MTBE	1.24	−29.34 ± 0.20[a]	−29.57 ± 0.15	−29.43 ± 0.25 $m = 10$	>0.95	−0.09 ± 0.45	<0.85	not significant
benzene	2.13	−27.45 ± 0.14	−27.49 ± 0.08	−26.36 ± 0.10 $m = 10$	0.75 ± 0.02[b]	1.09 ± 0.24	1.68	1.00044 ±0.00010
toluene	2.73	−28.86 ± 0.09	−28.74 ± 0.14	−27.66 ± 0.10 $m = 4$	0.50 ± 0.02	1.20 ± 0.19	2.12	1.00060 ±0.00010

[a] The range of dispersion given for the $\delta^{13}C$ values corresponds to ±2 standard deviations of the mean value $\sigma(\bar{X})$ of 10 measurements. [b] The range of dispersion given for $X_{freely\ dissolved}$ values corresponds to the standard deviation of the single values through all the sorption steps $\sigma(X)$.

isotopomer and one $^{13}C_1$-isotopomer containing one ^{13}C-atom, regardless of its position in the carbon skeleton. From the isotope ratios $R = C^{13C}/C^{12C}$ measured for the freely dissolved analyte fractions, the isotope fractionation factor $\alpha_{sorption}$ can be calculated using the eqs 2 or 4 (for derivation cf. ref *15* and the Supporting Information to this paper).

$$\alpha_{sorption} = \frac{K_{OC}^{12C}}{K_{OC}^{13C}} = \frac{1 - X_{freely\ dissolved}}{(R_{water}/R_{HA})^{1/m} - X_{freely\ dissolved}} \quad (2)$$

$$\delta^{13}C_{sample} = 1000 \cdot \frac{R_{sample} - R_{standard}}{R_{standard}} \quad (3)$$

$$\alpha_{sorption} \approx 1 + \Delta\delta^{13}C/[1000m(1 - X_{freely\ dissolved})] \quad (4)$$

$\delta^{13}C_{HA}$ and $\delta^{13}C_{water}$ correspond to the carbon isotope composition of the freely dissolved analyte fractions in the HA suspension and in the pure aqueous solution, respectively, in the conventional δ-notation (eq 3). $R_{standard}$ in eq 3 is the isotope ratio of the reference carbon source (Vienna Pee Dee Belemnite (*12*)). Equation 4 is used for calculating the fractionation factor $\alpha_{sorption}$ from the shift in the carbon isotope composition $\Delta\delta^{13}C = \delta^{13}C_{final\ state} - \delta^{13}C_{initial\ state}$ during a multistep batch experiment, in which a bound fraction is repeatedly produced and removed from the system. *m* is the number of identical sorption steps with $(1 - X_{freely\ dissolved})$ as the degree of analyte binding in each step. The aim of the multistep batch experiment was to generate a maximum isotope shift ($\Delta\delta^{13}C$) combined with a still-acceptable depletion of analytes in the final solution. According to eq 4, this aim can be better achieved by a large number of sorption steps rather than by high degrees of analyte binding per step. In practice a compromise must be made, i.e., a limited number of steps.

The isotope fractionation during the partitioning between humic substances and the water phase was investigated using benzene and toluene as model compounds. No distinction was made here between analyte interactions with dissolved and particulate organic matter. Table 1 summarizes the isotope composition of the freely dissolved analyte fractions, the calculated sorption coefficients (K_{OC}), and the calculated fractionation factors ($\alpha_{sorption}$).

MTBE does not significantly bind to the HA. As therefore expected, its isotope composition is neither affected by the sequence of sorption steps nor by the blank procedure. Benzene and toluene interact with the HA giving rise to 25% and 50% of bound fractions, respectively. The resulting sorption coefficients K_{OC} are reasonable (log K_{OW} − log K_{OC} ≈ 0.5). After 10 and 4 sorption steps (for benzene and toluene, respectively), the freely dissolved concentrations decrease to less than 5% of their initial values due to the removal of the sorbed fractions ($0.75^{10} \approx 0.5^4 \approx 0.06$) and some additional losses (dilution and evaporation). The stronger-binding toluene reached first the lower concentration level where the sequence of sorption cycles had to be interrupted to ensure an accurate isotope analysis. The isotope composition of both analytes provides clear evidence of ^{13}C-enrichment in the residual fractions. According to eq 4, fractionation factors of $\alpha_{benzene} = 1.00044 \pm 0.00010$ and $\alpha_{toluene} = 1.00060 \pm 0.00010$ can be derived. As observed for MTBE, no significant isotope shifts appear for benzene and toluene in the blank experiments without the interaction with HA.

Harrington et al. (*7*) investigated the isotope fractionation of BTEX compounds during HPLC separation under RP conditions (RP-18 column, 60% methanol + 40% water as eluent, about 2500 theoretical plates). From the finding that it was not possible to resolve nonlabeled from completely ^{13}C-labeled isotopomers (benzene and toluene), the authors estimated a maximum value of the transformed isotope fractionation factor as $|1 - \alpha_{sorption}| \leq 0.014$ for benzene and ≤ 0.012 for toluene. Obviously, the sensitivity of this approach was not sufficient to reveal the real fractionation effects, which are a factor of 20−30 smaller.

Slater et al. (*8*) and Schueth et al. (*9*) studied isotope fractionation of some chlorinated ethenes and BTEX compounds during sorption onto various carbonaceous materials (graphite, activated carbon, lignite coke, and lignite) by means of single-step batch experiments. In general, fractionation effects were in the range of the reproducibility limit of the analytical techniques (±0.5‰ for $\delta^{13}C$) under equilibrium conditions as well as for rate-limited sorption. Our results are in agreement with the experimental findings of Slater et al. (*8*) and Schueth et al. (*9*) insofar as single-step batch experiments are a priori unable to reveal the very small effects. Although in both reports the upper limits of possible fractionation factors were not estimated on the basis of a strict error consideration, they conclude that isotopic values of dissolved VOCs will not be significantly affected by equilibrium sorption in the subsurface (*8*). Schueth et al. (*9*) considered the analogy between contaminant transport in aquifers and HPLC columns. Comparing the number of theoretical plates in the two matrixes (about 0.7 m^{-1} in the Borden site aquifer in Canada and 10^5 m^{-1} in a typical HPLC column) and several other conditions, they came to the conclusion that, for typical plume lengths of some tens or hundreds of meters, sorption processes in aquifer systems are conservative with respect to isotope effects (*9*). This conclusion, however, is not necessarily justified by the available data, as will be presented in the following part of this paper.

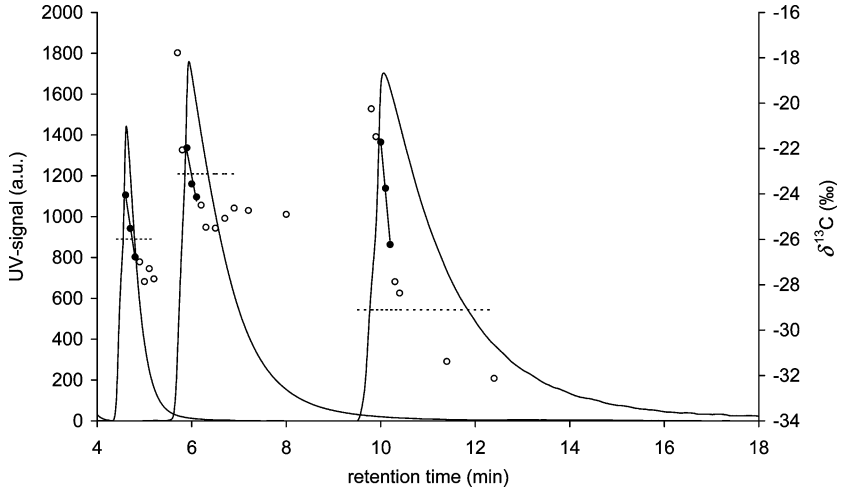

FIGURE 1. Superimposed chromatograms of benzene, 2,4-dimethylphenol, and *o*-xylene together with their isotope composition along the peak shapes (1 mL min^{-1} water, pH 5, 10 mM NaCl, humic-acid-coated column). The filled circles and straight lines correspond to the linear regression according to eq 6. The dashed lines correspond to the δ^{13}C-values of the nonfractionated analytes. The range of dispersion of the δ^{13}C-values is 0.5‰ (2 $\sigma(\bar{X})$).

Chromatographic Experiments. To measure carbon isotope effects of sorption more sensitively, chromatographic experiments involving a large number of successive sorption and desorption steps were conducted. Hydrophobic compounds were eluted through a HA-coated HPLC column with water to simulate partitioning within an aquifer as realistically as possible. The chromatographic peaks were separated into individual fractions and the isotope composition of the analytes was determined by GC−C−IRM−MS analysis. Typical chromatograms from the HA column are presented in Figure 1.

The elution profiles obtained are not optimal from the chromatography point of view. Nevertheless, significant carbon isotope fractionation is evident between the front and the back of the peaks; up to 4, 8, and 13‰ for benzene, 2,4-dimethylphenol, and *o*-xylene, respectively. The heavy isotopomers always move faster. This means that $K_{OC}^{12C} > K_{OC}^{13C}$ and consequently $\alpha_{sorption} > 1$. The present findings are consistent with the results of Caimi and Brenna (*10*, *11*) who found a shift of the isotope composition up to 5‰ across a methyl palmitate peak. Their results are remarkable from two points of view: (i) the isotope fractionation was obtained under low-performance RP−LC conditions (RP-8 preparative-scale column, acetonitrile), and (ii) the effect of one ^{13}C-atom per analyte molecule is attenuated by dilution with 16 ^{12}C-atoms in methyl palmitate. The ^{13}C-isotopomers eluted first. The course of the δ^{13}C value across the peak was similar to our findings: a sharp drop at the front edge followed by a slight decrease over the rest of the peak.

The concentration profile of an ideal chromatographic peak can be described as a Gaussian distribution.

$$C_{total} \approx q\frac{1}{\sqrt{2\pi} \times \sigma} \exp\left(-\frac{(t - t_{max})^2}{2\sigma^2}\right) \quad (5)$$

Herein, q is a parameter which describes the ratio of the injected amount of analyte to the eluent flow rate ($q = n_{analyte}/\dot{V}$), σ is the variance of the distribution, and t and t_{max} are the time variable and its value at the peak maximum, respectively.

Deviations from a Gaussian peak shape can be clearly seen with the HA column and water as eluent. They are due to nonideal partitioning behavior within the column giving rise to considerable tailing of the peaks. Experiments with a commercial RP-18 column (chromatograms not presented in this paper) produced similar results (extensive peak tailing) when pure water was used as eluent, but nearly Gaussian-shaped peaks without significant tailing were produced when acetonitrile−water mixtures were used. Therefore, we assume that the peak tailing is at least partly due to the eluent rather than an imperfect chromatographic apparatus or the HA column. Pure water is known to be an unfavorable eluent in the RP−HPLC (*16*). Nevertheless, we decided to accept the imperfect peak shapes in favor of a more realistic simulation of aquifer conditions, in particular to take into account the polarities of the original mobile and stationary phases.

Under the assumption that the region around the peak maximum is less affected by nonideal effects, the isotope composition of these fractions was used to calculate a linear regression curve according to eq 6.

$$\delta^{13}C_{sample} = -at + b \quad (6)$$

It can be shown that this approximation follows from the superposition of two adjacent Gaussian peaks, one of a ^{12}C- and the other of a ^{13}C-isotopomer (*15*). The selection of the data points for the linear regression in Figure 1 is not strictly defined. We followed the rule that all the nonideal chromatographic effects tend to damp the separation of isotopomers. Therefore, the highest slope of the regression line should be the most accurate. Rearranging eq 3 according to the definition of the δ-notation, the course of the two isotopomer peaks can be described by eqs 7 and 8.

$$C^{13C} = C_{total} \cdot \frac{1}{1 + \frac{1}{\left(1 + \frac{\delta^{13}C_{sample}}{1000}\right) R_{standard}}} \quad (7)$$

$$C^{12C} = C_{total} - C^{13C} = C_{total} \cdot \left(1 - \frac{1}{1 + \frac{\delta^{13}C_{sample}}{1000}}\right) R_{standard} \quad (8)$$

The $\delta^{13}C_{Sample}$ values in eqs 7 and 8 were replaced with eq 6. To determine the peak maxima of the ^{13}C- and ^{12}C-isotopomers eqs 7 and 8 were differentiated with respect to the retention time (t). The zero points of the first derivatives at $t = t_{max}$ were found by numerical approximation (Table 2). Introducing these calculated retention times t_{max} for the ^{12}C- and ^{13}C-isotopomer peaks into eq 5 and using $q^{12C} = (0.989\ n_{analyte})/\dot{V}$ and $q^{13C} = (0.011\ n_{analyte})/\dot{V}$, theoretical

TABLE 2. Calculated Retention Times (t_{max})[a] of Carbon Isotopomer Peaks for Three Analytes (Humic-Acid-Coated Column, Eluent: Water at pH 5, 10 mM NaCl) and Resulting Fractionation Factors ($\alpha_{sorption}$)

analyte	t_{max}^{12C} (min)	t_{max}^{13C} (min)	log K_{OW} (from lit.)	$\alpha_{sorption}$ (from eq 9)
benzene	4.61800	4.61756	2.13	1.00017
2,4-dimethylphenol	5.94801	5.94663	2.35	1.00035
o-xylene	10.07708	10.06950	3.12	1.00092

[a] Retention time of the conservative tracer (KNO_3) is t_d = 2.02 min.

isotope concentration profiles can be calculated which include the corresponding δ^{13}C-curves along the elution profile. From the net retention times t_r of the two isotopomer peaks ($t_r = t_{max} - t_d$ with t_d = 2.02 min for nitrate as a conservative tracer), the isotope fractionation factor ($\alpha_{sorption}$) can be calculated according to eq 9.

$$\alpha_{sorption} = \frac{K_d^{12C}}{K_d^{13C}} = \frac{K_{OC}^{12C}}{K_{OC}^{13C}} = \frac{t_r^{12C}}{t_r^{13C}} \quad (9)$$

The ratio of the total distribution coefficients (K_d) can be substituted by the ratio of the corresponding K_{OC} values, because partitioning between the mobile water phase and the stationary HA phase is by far the dominant retardation mechanism for hydrophobic compounds. Compared to nitrate, benzene, 2,4-dimethylphenol, and *o*-xylene were retarded by factors of 2.28, 2.95, and 5, respectively. With increasing retardation of the compounds, the individual peak shapes show more nonideal elution behavior.

Although extracted from dynamic experiments, the fractionation factor $\alpha_{sorption}$ has the same mechanistic meaning as in batch experiments: it is the ratio of the sorption coefficients of two carbon isotopomers. This assumes that local sorption equilibria are actually established. This condition was confirmed by variation of the eluent flow rate (0.2 to 2.0 mL min^{-1}), which did not change the retention factor of benzene significantly (2.28 ± 0.02). The chromatographic procedure is only a means to amplify the fractionation effect, i.e., to make it more easily measurable. Therefore, the calculated $\alpha_{sorption}$ values in Table 2 can be directly compared with those from the batch experiments given in Table 1. Although for benzene the two values are not identical ($1000 \cdot |1 - \alpha_{sorption}|$ = 0.17 vs 0.44 ± 0.10), all the values are in the same order of magnitude ($1000 \cdot |1 - \alpha_{sorption}|$ = 0.17−0.92 from the chromatographic data vs 0.44−0.60 from the batch experiment). When making this comparison, the quite different experimental conditions and calculation procedures applied for extracting the fractionation factors ($\alpha_{sorption}$) must be taken into account. Although the detectable isotope shifts are higher with the chromatographic method, the assumptions and approximations introduced into the data analysis make the calculated fractionation factors susceptible for biases. As an example, if the number of data points in Figure 1 selected for the linear regression (eq 6) were changed, the slope (*a*) may vary significantly (±25%). The transformed fractionation factor $1000 \cdot |1 - \alpha_{sorption}|$ varies approximately proportional to the value of *a*. Therefore, we consider them as reasonable estimates rather than precise values. In contrast, the batch experiments produce a small isotope shift, but the data analysis is simple and straightforward. Therefore, the two approaches can complement each other.

The expression $\alpha_{sorption} > 1$ means that the ^{12}C-isotopomers interact more strongly with the HA and are thus more retarded than the ^{13}C-isotopomers. This is the same trend as observed for the evaporation of BTEX-aromatics (*7*) and trichloroethene (*17*). The heavy isotopomers are enriched in the vapor phase relative to the liquid solvent phase. This is termed an inverse isotope effect. The data are consistent with the fractionation factors $\alpha_{liquid-vapor} = p^{12C}/p^{13C}$ = 0.99980 ± 0.00003 for BTEX-aromatics and $\alpha_{liquid-vapor}$ = 0.99930 ± 0.00005 for trichloroethene. All these sorption and evaporation-based isotope fractionations obey the same rule, that "van der Waals interactions with the nonpolar component of the column (or the nonpolar solvent phase) are reduced for the heavy isotopomers" (*11*). It is remarkable that the fractionation factors for vapor condensation and hydrophobic sorption from water are similar (e.g., $1/\alpha_{liquid-vapor} \approx \alpha_{sorption}$). An explanation could be that both fractionation processes are driven by the same force: nonspecific hydrophobic (van der Waals) interactions. In contrast, evaporation of the same compounds from an aqueous solution is not affected by carbon isotope fractionation ($\alpha_{aqueous\ solution-vapor} \approx 1$) (*13*). This is consistent with the proposed explanation because hydrophobic interactions do not play a significant role in the two phases: the aqueous solution and the vapor phase.

The fractionation factors given in Tables 1 and 2 tend to increase with rising hydrophobicity of the analytes, expressed as peak retention times (t_{max}) and log K_{OW}. However, such a correlation is not necessarily valid. The values for benzene and toluene from batch experiments are not significantly different. For the chromatographic data, we cannot rule out that part of this tendency may be due to the increasing divergence of the chromatographic peaks for 2,4-dimethylphenol and *o*-xylene from the Gaussian shape.

Development of a Model to Estimate Effects of Hydrophobic Sorption on Isotope Composition of Contaminants in Aquifers. Isotope fractionation due to hydrophobic sorption was verified in laboratory experiments designed to examine whether the retarded transport of organic contaminants within an aquifer may affect their isotope composition. To estimate the extent of fractionation occurring in aquifers, it is useful to consider some characteristic parameters of chromatographic separation systems in order to make aquifers and HPLC columns comparable (for basics of chromatographic theory see various handbooks, e.g., ref *18*).

The retardation of any compound in a chromatographic system, regardless of whether it is an aquifer or an HPLC column, can be described by the retardation factor $\mathscr{R}$. This is the ratio between the average migration velocities (u in m s^{-1}) of a conservative, i.e., nonretarded tracer ($u_{tracer} = u_{eluent}$) and of the retarded analyte. $\mathscr{R}$ can be calculated from eq 10 using some characteristic properties of the aquifer and the analyte.

$$\mathscr{R} = \frac{u_{tracer}}{u_{analyte}} = 1 + \frac{1-\epsilon}{\epsilon} \cdot K_{OC} \cdot f_{OC} \cdot \rho_{solid} = 1 + f_\epsilon \cdot K_{OC} \quad (10)$$

ϵ is the aquifer porosity, f_{OC} is the fraction of organic carbon in the solid aquifer matrix (frequently in the order of 0.0001 to 0.01 g of OC per g of solid material), ρ_{solid} is the density of the solid bulk phase (kg L^{-1}), and K_{OC} is the organic-carbon-normalized sorption coefficient of the analyte (L kg^{-1}). The aquifer properties $\rho_{solid} \cdot f_{OC} \cdot (1-\epsilon)/\epsilon$ are consolidated into f_ϵ [kg L^{-1}] in eq 10.

A second important parameter of the chromatographic system is its separation efficiency, which can be described by the number of theoretical plates (N). N may be expressed as the product of the number of theoretical plates per meter (N') and the length of the separation distance (L): $N = N' \cdot L$. L can be understood to be the length of a contaminant plume in the case of continuous contaminant feeding or as the peak migration distance in the case of a point contamination event. N is related to the variance (σ) of an ideal Gaussian-shaped chromatographic peak (or to its width at half of the peak

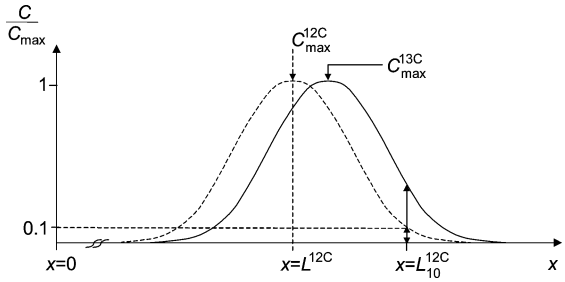

FIGURE 2. Schematic presentation of the chromatographic separation of ^{12}C- and ^{13}C-isotopomers of a contaminant in an aquifer along the groundwater flow direction after a short contamination event. Concentrations are normalized to the maximum total carbon concentration (C_{max}). The concentration of the ^{13}C-isotopomer is amplified by a factor of 99. L_{10}^{12C} is the length coordinate of the peak front where the concentration of the contaminant's ^{12}C-isotopomers has decreased to 10% of its maximum value.

height $\Delta t_{1/2} = 2.35\ \sigma$). The relation between the peak width (σ), number of theoretical plates (N), peak retention time (t_{max}), peak migration distance (L), groundwater flow velocity (u), and the retardation factor ($\mathscr{R}$) is given by eq 11.

$$\sigma^2 = \frac{t_{max}^{\ 2}}{N} = \frac{\left(\frac{L}{u}\cdot\mathscr{R}\right)^2}{N'\cdot L} = \frac{L}{N'}\cdot\left(\frac{\mathscr{R}}{u}\right)^2 \tag{11}$$

To make the processes in the two systems—chromatographic column and aquifer—more comparable, the parameter retention time (t) is converted into a distance parameter (x) according to $t - t_{max,i} = (x - L_i)\cdot \mathscr{R}_i/u$ with i as the index of analyte i and $x = 0$ as the position of the contaminant source. This makes it possible to transform the time scale of the column experiment ($t - t_{max}$ in eq 5) into the aquifer domain, where a plume distance ($x - L$) at a certain time is typically considered. The isotope fractionation of an idealized peak after a short contamination event at time $t = 0$ and at the place $x = 0$ due to chromatographic separation of two isotopomers will lead to an enrichment of heavy isotopomers at the front of the migrating peak (Figure 2).

The transformation of the time scale in Figure 1 into the distance scale in Figure 2 makes the sequence of isotopomers appear to be reversed. In fact, the heavy isotopomer moves faster in both cases.

Using eq 11 and introducing $(t - t_{max,i}) = (x - L_i)\cdot \mathscr{R}_i/u$ into eq 5 results in eq 12, which describes the one-dimensional dispersion of the contaminant (i) along the groundwater flow as a function of the distance (x) from the source point.

$$C_{total} \approx q\cdot \frac{\sqrt{N'}\cdot u}{\sqrt{2\pi\cdot L}\cdot\mathscr{R}}\cdot\exp\left(-\frac{N'\cdot(x-L)^2}{2L}\right) \tag{12}$$

Eq 12 can be applied to any contaminant, including isotopomers of the same contaminant. When applying the formulas, it is helpful to be aware of the fact that the ratio of the retardation factors of two isotopomers $\mathscr{R}_i^{12C}/\mathscr{R}_i^{13C}$ can sometimes be approximated as 1, whereas the difference $\mathscr{R}_i^{12C} - \mathscr{R}_i^{13C}$ always has to be accounted for.

Dividing eq 12 for the two isotopomers, using $L_i^{13C} = L_i^{12}\cdot(\mathscr{R}_i^{12C}/\mathscr{R}_i^{13C})$ and the approximation $\sigma^{13C} \approx \sigma^{12C}$, results in eq 13, which describes the isotope composition of the contaminant plume (R_x) as a function of the distance parameter (x).

$$R_x = \frac{(C^{13C})_x}{(C^{12C})_x} \approx R_0\cdot\exp\left[\frac{N'}{2\cdot L^{12C}}\left(\frac{1 + K_{OC}^{12C}\cdot f_\epsilon}{1 + K_{OC}^{12C}\cdot f_\epsilon/\alpha_{sorption}} - 1\right)(x^2 - (L^{12C})^2)\right] \tag{13}$$

R_0 corresponds to the isotope ratio of the carbon in the starting compound before the fractionation process. Important parameters responsible for the degree of fractionation are the fractionation factor ($\alpha_{sorption}$) which can be determined in laboratory experiments, the magnitude of contaminant retardation ($K_{OC}\cdot f_\epsilon$) which can be estimated from contaminant properties (e.g., K_{OW}), the organic carbon content of the aquifer material (f_{OC}) and the plume length ($L_{total} \approx L^{12C}$). A crucial parameter is the specific number of theoretical plates in the aquifer. From tracer experiments in our laboratory with an undisturbed sediment column from a sandy aquifer material we estimated $N' \approx 3\ m^{-1}$. Schueth et al. (9) estimated $N' \approx 0.54-0.74\ m^{-1}$ from in situ experiments with CCl_4 and C_2Cl_4 in the aquifer at the Borden site in Canada (travel time 633 d). This gives a rough estimate of the separation efficiency of natural aquifer materials.

Having experimentally determined or reasonably assumed values for all the parameters in eq 13, one can calculate the carbon isotope profile along the moving contaminant plume. It seems reasonable to approximate the front of a migrating plume in a manner similar to the edge of a moving contaminant zone. As an example, the migration of benzene in an aquifer was simulated, whereby some key parameters ($f_{OC} = 0.0005$ and 0.005, $N' = 0.5-5.0\ m^{-1}$, $L = 100$ and 500 m) were varied and other parameters ($K_{OC} \approx 0.5\cdot K_{OW} = 67$ L kg^{-1}, $\rho_{solid}\cdot(1 - \epsilon)/\epsilon = 4$ kg L^{-1}) were kept constant. The assumed parameter sets are plausible values for BTEX plumes in contaminated sandy aquifers. Let us consider the isotope composition of the pollutant at a certain distance ahead of a peak maximum. This distance is defined by the ratio of the local pollutant concentration (C) relative to its maximum concentration (C_{max}). The corresponding distance parameter ($L_{Cmax/C}^{12C}$) can be calculated with eq 14, which is simply derived from eq 12.

$$L_{Cmax/C}^{12C} = L^{12C} + \sqrt{\frac{2}{N'}\cdot L^{12C}\cdot\ln\frac{C_{max}}{C}} \tag{14}$$

Introducing $x = L_{Cmax/C}^{12C}$ into eq 13 leads to the isotope composition of the pollutant at that position. The isotope shift in the pollutant peak between the positions $x = L^{12C}$ and $x = L_{Cmax/C}^{12C}$, i.e., in the peak maximum and its forerunning flank, are expressed as $\Delta\delta^{13}C$ values according to eqs 15 and 16.

$$\Delta\delta^{13}C = \frac{R_{x=L_{Cmax/C}} - R_{x=L}}{R_{standard}}\cdot 1000\ ‰ \tag{15}$$

$$\Delta\delta^{13}C = 1000‰\cdot\frac{R_0}{R_{standard}}\cdot\left\{\exp\left[\ln\frac{C_{max}}{C}\cdot\left(\sqrt{\frac{2N'\cdot L^{12C}}{\ln(C_{max}/C)}} + 1\right)\left(\frac{1 + K_{OC}^{12C}\cdot f_\epsilon}{1 + K_{OC}^{12C}\cdot f_\epsilon/\alpha_{sorption}} - 1\right)\right] - 1\right\} \tag{16}$$

From the structure of eq 16 it is obvious that the parameters $N'\cdot L$ and $K_{OC}\cdot f_\epsilon$ can be grouped together. Altogether, eq 16 contains 4 characteristic parameters which determine the predicted extent of spatial isotope fractionation: $\alpha_{sorption}$, C_{max}/C, $N'\cdot L = N$, and $1 + K_{OC}\cdot f_\epsilon = \mathscr{R}$. They are the fractionation

TABLE 3. Shift of Carbon Isotope Composition $\Delta\delta^{13}C$ of Benzene along the Forerunning Flank of a Chromatographic Peak ($C_{max}/C = 10$) Migrating through an Aquifer, Calculated According to Eqs 13−16 (Applied Parameters: $K_{OC} = 67$ L kg^{-1}, $\alpha_{sorption} = 1.00017$, $\rho_{solid} = 2.67$ kg L^{-1}, $\epsilon = 0.4$)

L (m)	N' (m^{-1})	$N = N' \cdot L$	L_{10}^{12C} (m)	f_{OC}	$\Delta\delta^{13}C$ (‰) between $x = L$ and $x = L_{10}^{12C}$
100	0.5	50	130.3	0.0005[a]	0.37
500	0.5	250	567.9	0.0005	0.74
100	2.5	250	113.6	0.0005	0.74
500	2.5	1250	530.3	0.0005	1.56
100	5.0	500	109.6	0.0005	1.01
500	5.0	2500	521.5	0.0005	2.17
100	0.5	50	130.3	0.005[b]	1.69
500	0.5	250	567.9	0.005	3.47
100	2.5	250	113.6	0.005	3.47
500	2.5	1250	530.3	0.005	7.47
100	5.0	500	109.6	0.005	4.81
500	5.0	2500	521.5	0.005	10.47

[a] $\mathscr{R} = 1.13$. [b] $\mathscr{R} = 2.34$.

factor, a measure of the observation position along the front edge of the plume, the number of theoretical plates, and the retardation factor, respectively. This means that a lower separation efficiency of an aquifer may be compensated for by a larger plume length and that a lower OC content of the aquifer material is compensated for by a higher sorption tendency of the sorbate.

The results of the calculations according to eq 16 are summarized for benzene in Table 3. For these calculations, the conservative estimate of the fractionation factor $\alpha_{sorption} = 1.00017$ from the dynamic experiments was applied. The predicted effects would be even larger with $\alpha_{sorption} = 1.00044$ as obtained from the batch experiment.

In Table 3 and Figure 2 we have arbitrarily chosen that point of observation where the concentration of the pollutant is down to 10% of its maximum value ($C_{max}/C = 10$, $x = L_{10}^{12C}$).

The simulation shows that the organic carbon content of the aquifer matrix ($f_{OC} \sim f_\epsilon$) and the number of theoretical plates along the contaminant path ($N = L \cdot N'$) have pronounced effects on the spatial isotope shift ($\Delta\delta^{13}C$). The carbon isotope composition can be significantly altered by up to several δ‰-units. For identical fractionation factors ($\alpha_{sorption}$) and aquifer parameters, the isotope shift increases with increasing sorption tendency (K_{OC}) of the pollutant. Therefore, one can predict even larger isotope shifts for pollutants which are more hydrophobic than benzene.

To illustrate the effect of sorption on isotope fractionation of more hydrophobic compounds, 2,4-dimethylphenol and *o*-xylene were examined. The aquifer parameters applied in these calculations are as follows: $L^{12C} = 100$ m, $f_{OC} = 0.0005$, $N' = 2.5$ m^{-1}, $f_\epsilon = 4$ kg L^{-1}. The applied compound properties are $K_{OC} = 112$ L kg^{-1}, $\alpha_{sorption} = 1.00035$ for 2,4-dimethylphenol, and $K_{OC} = 660$ L kg^{-1}, $\alpha_{sorption} = 1.00092$ for *o*-xylene. Considering a migration distance of 100 m, from eq 16 isotope shifts of 2.2 and 18.5‰ are estimated between the peak maxima and the 10% concentration intersections at 113.6 m. If we presume that the fractionation factors of these compounds are possibly overestimated due to strong peak-tailing in the HPLC experiments, a strictly conservative estimate can be based on the minimum fractionation factor of benzene ($\alpha_{sorption} = 1.00017$). Equation 16 then predicts a lower isotope shift for *o*-xylene of $\Delta\delta^{13}C = 3.5$‰, which, however, is still quite significant. In this case, the larger isotope shift of *o*-xylene compared with benzene ($\Delta\delta^{13}C = 0.74$‰) is exclusively the result of its higher sorption tendency (K_{OC}).

Implications for Environmental Studies. The isotope shift between the center of a contaminant plume and its preceding edge has been interpreted as an indication of in situ biodegradation. Under certain conditions (*4, 5*), the Rayleigh equation (eq 17) can be applied to estimate the degree of degradation from the isotope shift between the starting and the remaining contaminant fraction.

$$\frac{C_t}{C_0} = \left(\frac{R_t}{R_0}\right)^{\alpha/(1-\alpha)} \tag{17}$$

C_t and C_0 are the remaining and the initial contaminant concentrations, respectively. R_t and R_0 are the corresponding carbon isotope ratios. α is the fractionation factor of the degradation process. Taking a reasonable value of $\alpha_{reaction} = 1.002$ for the biodegradation of BTEX compounds under anoxic conditions (*5*) and a predicted sorption-based isotope shift of *o*-xylene ($\Delta\delta^{13}C = 3.5$‰, conservative model estimation, conditions as described above) results in an apparent degree of biodegradation of 82.6%, which did not take place in this case. Hydrophobic sorption and biodegradation shift the carbon isotope signature of the preceding (remaining) contaminant fraction in the same direction: the heavy isotopomers are enriched. Obviously, sorption-based isotope fractionation effects may be quantitatively relevant for interpreting carbon isotope signatures.

As a rule, the magnitude of the kinetic carbon isotope effect $\alpha_{reaction} = k^{12C}/k^{13C}$ may be expected to decrease with rising number of carbon atoms in the molecule. This follows from the statistical point of view, if we define the rate constants on the molar basis (rather than on the atom basis) and for naturally occurring carbon. In contrast to this tendency, we have some indications that the sorption isotope effect $\alpha_{sorption}$ becomes more pronounced with increasing hydrophobicity, i.e., with increasing number of carbon atoms in the molecule. Furthermore, according to eq 16 the magnitude of $\Delta\delta^{13}C$ will increase with increasing hydrophobicity (K_{OC}) of the solute. Considering the three tendencies together, the importance of isotope effects caused by sorption in relation to those caused by reactions might increase for more hydrophobic organic compounds, such as polycyclic aromatic hydrocarbons. This hypothesis requires further experimental examination.

Regarding real contaminated aquifers, it is useful to consider two different scenarios as follows: (1) The scenario of a migrating contaminant front within an aquifer, similar to a chromatographic elution, may be realistic when a single spill of dissolved contaminants is entering the aquifer or when a finite plume is migrating within an aquifer. According to our results, in this case the front of the contaminant plume can be enriched in heavy carbon isotopomers due to sorption-based isotope fractionation. This certainly has to be taken into account when isotope fractionation is taken as an indicator to assess in situ biodegradation. (2) Many aquifer contaminations, however, are the result of point sources which consist of free nonaqueous-phase liquid (NAPL) phases, whereby the flowing groundwater leaches contaminants, forming a continuously fed plume. In this scenario, chromatographic effects can be expected to affect the composition of the migrating front, whereas in the core of the plume the chemical and isotope signatures should be very similar to those of the source. This approximation may be illustrated by considering the plume to be composed of an infinite number of distinct chromatographic peaks, which all have sorption-affected fronts and tails, whereby the isotope depletion and enrichment of the overlapping fronts and tails compensate each other.

For further considerations, it is useful to distinguish between isotope fractionation in stationary and nonstationary plumes. Stationary plumes ("old plumes") are defined as

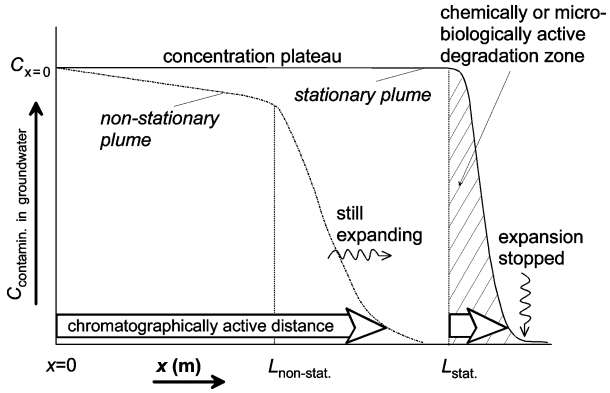

FIGURE 3. One-dimensional schematic presentation of the stationary and nonstationary contaminant plume scenarios.

those which have already achieved an equilibrium between contaminant delivery and chemical elimination rates, giving rise to a stationary plume length. Nonstationary ("young") plumes are those which are still expanding. Figure 3 contains a schematic presentation of the two scenarios, which are of course strongly idealized in order to make the significant concepts clear.

In nonstationary plumes, the entire plume length acts as a chromatographic column and determines the number of available theoretical plates. All estimations discussed above are valid in this scenario. Under stationary conditions, the effective length of the "separation column" is only the distance between the end of the plume core and the point of observation in the front profile. Hence, the degree of isotope fractionation due to sorption will be smaller and possibly insignificant. A more detailed rationale of these conclusions is given in the Supporting Information.

What are the principal effects of simultaneous sorption and degradation processes with respect to the spatial isotope signature? We will discuss two nonchromatographic effects, the "residence time effect" and the "availability effect". (1) Heavy isotopomers move faster in the aquifer than light isotopomers. Thus, the available reaction time between two measuring points (e.g., aquifer wells) is shorter. Their degree of degradation between these points is smaller. The enrichment of heavy isotopomers at the tip of the plume is reinforced. (2) Hitherto we have only considered total concentrations of contaminants, regardless of their phase speciation. For various degradation processes it may be important whether the contaminant molecules are in the dissolved or in the sorbed state. It is reasonable to assume that microbial transformations proceed preferentally with dissolved substrates. Hence, different sorption affinities (K_{OC}) of light and heavy carbon isotopomers will affect their availability for degradation processes. The less sorbing heavy isotopomers are degraded faster.

It is important to stress here that the conclusions about these two impacts—the "residence time effect" and the "availability effect"—are not based on any assumptions about the efficiency of chromatographic separation in an aquifer. They are due to the different extent of sorption of the light and the heavy isotopomers at any place in the aquifer. This means that they are independent of the plume length and the aquifer separation efficiency (N'), which both may be subject to a large degree of uncertainty in real aquifers. If it is the case that $|1 - \alpha_{sorption}| \ll |1 - \alpha_{reaction}|$, then the nonchromatographic sorption impacts of the sorption-based isotope effects may possibly be negligible, because they are not amplified by a number of successive separation steps as discussed above. If, however, the sorption fractionation factor of hydrophobic contaminants is close to the magnitude of the kinetic fractionation factor, e.g., for *o*-xylene $\alpha_{sorption} \leq 1.001$ vs $\alpha_{reaction} \approx 1.002$, even the nonamplified sorption impacts may become significant.

We are aware of the fact that all these isotope-based effects are small compared with mixing effects due to the heterogeneity of real aquifers. Nevertheless, significant isotope shifts are observed along real contaminant plumes, which need to be understood (*4*, *5*, *19*, *20*). However, it is difficult to verify our model predictions by means of field data, because usually retardation factors of the pollutants are not available. Thus, the potential effect of sorption on contaminant retardation and the possible degree of isotope fractionation cannot be estimated. Moreover, possible superposition of sorption, biodegradation, and flow segregation due to aquifer heterogeneity (see below) make an unambiguous interpretation of field data difficult.

Very recently, results of a tracer field test with toluene under well-defined conditions (a sandy gravel aquifer at a former industrial site near Zeitz, East Germany, $f_{OC} \approx 0.0015$, $N' \approx 0.7-1.0\ m^{-1}$, strictly anaerobic, contaminated with benzene) have been published (*21*). Surprisingly, the observed retardation factor of toluene ($\mathscr{R}_{observed} \approx 1.1$, determined versus bromide as conservative tracer) was much lower than predicted from the OC content of the aquifer material ($\mathscr{R}_{predicted} \approx 2.5$). This means that hydrophobic sorption plays only a minor role under these field conditions, although the OC content of the aquifer material lets us expect a significant retardation. Thus, sorption-caused isotope fractionation is not likely to be observed there. The reason of the low sorption efficacy of the organic matter is not clear.

Summarizing the available field data, we have to conclude that there is no clear evidence of sorption-based carbon isotope fractionation in real aquifers. Therefore, the relevance of this effect for real environmental scenarios remains a matter of discussion.

Implications of Aquifer Heterogeneity—the Segregation Problem. In addition to sorption-based isotope fractionation, another phenomenon may affect the relationship between measured isotope signatures and the degree of contaminant degradation. The practical problem lies in the fact that a decrease of contaminant concentration along the plume length is not by itself a sufficient indication of degradation processes. The isotope signature may provide additional information. Usually, the Rayleigh equation (eq 17) is applied to estimate degradation degrees from isotope shifts: it holds for homogeneous reaction media under certain conditions (*22*). However, real aquifers are more-or-less heterogeneous systems with strongly varying local reaction conditions. Figure 4 schematically illustrates the impacts resulting from this micro- and macroheterogeneity: let us consider a plume scenario with four equal segments of groundwater flow ($\dot{V}_1$ through $\dot{V}_4$) which pass different types of aquifer zones. The first groundwater flow segment passes through a zone which is very beneficial for chemical or microbial degradation (e.g. high concentration of Fe^{3+} as electron acceptor) which may result in a more-or-less complete transformation of the contaminant ($C_L = 0$), whereas the fourth flow segment passes through an almost inert aquifer zone with no significant transformation activity (e.g., a preferential flow path). Between these two extreme conditions, in the second and the third aquifer zones a partial biodegradation takes place ($C_L \approx {}^1/_2 C_0$ assumed). The second flow segment is considered to have uniform reaction conditions which give rise to a final carbon isotope fractionation of $\Delta\delta^{13}C = 1.39‰$ at 50% conversion. The third flow segment is considered to pass through a microheterogeneous aquifer zone where transformation of the contaminant may occur, but only within distinct microcompartments (e.g., pore volumes enriched with reactive Fe^{3+}).

If the reaction rate within these microcompartments is considerably higher than the mass transfer rate between the microcompartments and the bulk flow, then the transfor-

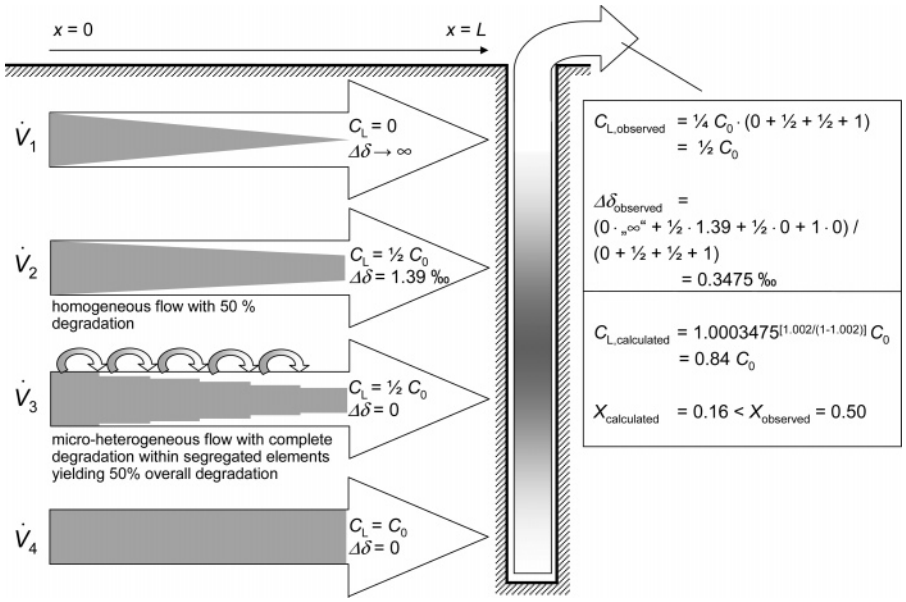

FIGURE 4. Effects of aquifer heterogeneity and groundwater mixing on observable isotope fractionation (arrows stand for groundwater flow segments, gray areas stand for contaminant concentrations, assumed: $\alpha_{reaction} = 1.002$, $\dot{V}_1 = \dot{V}_2 = \dot{V}_3 = \dot{V}_4$.

mation can become nearly complete within the microcompartments. However, only a fraction of the contaminant amount comes into contact with reactive compartments. The result of such a type of kinetics is a partial contaminant conversion with no observable isotope fractionation ($\Delta\delta^{13}C = 0$). Obviously, the isotope signatures of the flow segments 2 and 3 are significantly different despite the assumed equal overall degrees of conversion.

If the four groundwater flow segments reach a common point and unite (e.g., inside a monitoring well), the effective degree of degradation in the mixture is 50% (see Figure 4). The isotope shift of the nonconverted contaminant fraction in the mixture ($\Delta\delta^{13}C \approx 0.35$‰), however, is less than would be expected from a 50% conversion ($\Delta\delta^{13}C = 1.39$‰) in an uniform aquifer segment. The recalculation of an apparent degree of biodegradation from the observable carbon isotope shift by means of the Rayleigh equation gives $X_{calculated} = 0.16$, which is clearly lower than the actual value of $X_{observed} = 0.5$. This means an underestimation of the biodegradation in a heterogeneous aquifer.

The principal problem is well-known in the chemical engineering theory as "segregation of macrofluids" (*23*): it may have significant impacts on the kinetics and selectivity of chemical reactions. Implications of the segregation phenomenon for isotope patterns are examined in a more quantitative manner in ref *15*. The general conclusion from these considerations for the aquifer scenario is as follows: the segregation effect leads to an underestimation of degradation processes from isotope measurements which are difficult to quantify. However, it will never give rise to an overestimation of degradation processes.

Acknowledgments

We thank Dr. Katrin Mackenzie for preparing the humic-acid-coated HPLC material, Dr. Andrea Vieth for experimental support with GC−C−IRM−MS measurements, and Silke Woszidlo for experimental assistance (all three from UFZ Leipzig-Halle). We acknowledge the Federal Ministry of Education and Research for financial support (grant 02WT0022).

Supporting Information Available

Derivation of some of the applied equations. This material is available free of charge via the Internet at http://pubs.acs.org.

List of Symbols

α	isotope fractionation factor
$\alpha_{apparent}$	observed isotope fractionation factor
$\alpha_{liquid-vapor}$	equilibrium isotope fractionation factor for evaporation of solvents
$\alpha_{reaction}$	kinetic isotope fractionation factor of a chemical or microbial transformation
$\alpha_{sorption}$	isotope fractionation factor for sorption to organic matter
C	concentration [mol L^{-1}] or [mol kg^{-1}]
C_0	initial concentration of a compound [mol L^{-1}]
C^{12C}; C^{13C}	concentrations of ^{12}C and ^{13}C, respectively, [mol mol^{-1}] or [mol L^{-1}] or [at. % C]
$C_{analyte\ sorbed}$	analyte concentration on the sorbent [mol kg^{-1}]
C_{max}	maximum total carbon concentration of an analyte [mol L^{-1}]
C_{oc}	concentration of dissolved and particulate organic carbon in water [kg L^{-1}]
C_t	concentration of a compound remaining after the reaction time t [mol L^{-1}]
C_{total}	total concentration of carbon in [mol L^{-1}]
$\delta^{13}C$	delta notation of the isotope ratio of a compound [‰]
$\delta^{13}C_{HA}$	delta notation of the isotope ratio of the freely dissolved fraction of a compound in HA-containing solution [‰]
ϵ	aquifer porosity
f_ϵ	factor describing the ratio of organic carbon mass to water volume [kg L^{-1}] in a volume element of the aquifer
f_{OC}	mass fraction of organic carbon in soil or sediment

k^{12C}; k^{13C}	rate constants for the reaction of ^{12}C- and $^{13}C_1$-isotopomers, respectively, [s^{-1}]
K_d; K_d^{12C}; K_d^{13C}	distribution coefficients of a compound and of ^{12}C- and $^{13}C_1$-isotopomers, respectively, [L kg^{-1}]
K_{OC}; K_{OC}^{12C}; K_{OC}^{13C}	organic-carbon-normalized sorption coefficients of a compound and of ^{12}C- and $^{13}C_1$-isotopomers, respectively, [L kg^{-1}]
K_{OW}	octanol−water partition coefficient
L_i; L^{12C}; L^{13C}	migration distance of compound i and of ^{12}C- and $^{13}C_1$-isotopomers, respectively, [m]
$L_{Cmax/C}^{12C}$	distance in front of a plume or a peak [m] where the contaminant concentration (C) reaches a certain fraction of its maximum value (C_{max})
λ	wavelength [nm]
m	number of sorption steps in the multistep batch experiment
n	analyte amount [mol]
N	number of theoretical plates
N'	number of theoretical plates per meter [m^{-1}]
p^{12C}; p^{13C}	vapor pressure of ^{12}C- and $^{13}C_1$-isotopomers of a solvent
q; q^{12C}; q^{13C}	ratio of the amount of analyte (or ^{12}C− or $^{13}C_1$-isotopomers, respectively) injected into the HPLC system to the eluent flow rate [mol s L^{-1}]
R	carbon isotope ratio
R_0	carbon isotope ratio of the initial compound before the fractionation process
R_{HA}	carbon isotope ratio of the freely dissolved fraction of a compound in an HA-containing solution or suspension
R_{water}	carbon isotope ratio of a compound in pure aqueous solution
R_x	carbon isotope ratio of a compound at the dispersion distance x in an aquifer
$R_{standard}$	carbon isotope ratio of the reference material (VPDB)
$\mathscr{R}$; $\mathscr{R}^{12C}$; $\mathscr{R}^{13C}$	retardation factors of a compound and of ^{12}C- and $^{13}C_1$-isotopomers, respectively
ρ_{solid}	density of the solid bulk phase [kg L^{-1}]
σ	variance of a Gaussian distribution, [s] or [m]
t	time variable [s]
$\Delta t_{1/2}$	width at half of the peak height [s]
t_d	retention time of a conservative tracer [s]
t_{max}	retention time of the peak maximum [s]
t_r	net retention time [s]
Δt; Δt^{12C}; Δt^{13C}	migration time (between two measuring points in an aquifer) of a compound and of ^{12}C- and $^{13}C_1$-isotopomers, respectively, [s]
u	groundwater flow velocity [m s^{-1}]
$u_{analyte}$	average migration velocity of the analyte [m s^{-1}]
u_{eluent}	eluent flow velocity [m s^{-1}]
u_{tracer}	average migration velocity of a nonretarded tracer [m s^{-1}]
$\dot{V}$	eluent flow rate [L s^{-1}]
x	distance parameter [m] with $x = 0$ as the position of a contaminant source
$X_{freely\ dissolved}$	fraction of freely dissolved analyte, $X_{freely\text{-}dissolved} = n_{freely\ dissolved}/n_{total}$
X_{sorbed}	fraction of sorbed analyte, $X_{sorbed} = n_{sorbed}/n_{total}$
$X_{observed}$	observed (real) degree of conversion of a contaminant
$X_{calculated}$	degree of conversion calculated from the carbon isotope shift

Literature Cited

(1) Meckenstock, R. U.; Morasch, B.; Warthmann, R.; Schink, B.; Annweiler, E.; Michaelis, W.; Richnow, H. H. $^{13}C/^{12}C$ isotope fractionation of aromatic hydrocarbons during microbial degradation. *Environ. Microbiol.* **1999**, *1*, 409−414.

(2) Hunkeler, D.; Aravena, R.; Butler, B. J. Monitoring Microbial Dechlorination of Tetrachloroethene (PCE) in Groundwater Using Compound-Specific Stable Carbon Isotope Ratios: Microcosm and Field Studies. *Environ. Sci. Technol.* **1999**, *33*, 2733−2738.

(3) Ahad, J. M. E.; Sherwood Lollar, B.; Edwards, E. A.; Slater, G. F.; Sleep, B. E. Carbon Isotope Fractionation during Anaerobic Biodegradation of Toluene: Implications for Intrinsic Bioremediation. *Environ. Sci. Technol.* **2000**, *34*, 892−896.

(4) Sherwood Lollar, B.; Slater, G. F.; Sleep, B.; Witt, M.; Klecka, G. M.; Harkness, M.; Spivack, J. Stable Carbon Isotope Evidence for Intrinsic Bioremediation of Tetrachloroethene and Trichloroethene at Area 6, Dover Air Force Base. *Environ. Sci. Technol.* **2001**, *35*, 261−269.

(5) Richnow, H. H.; Anweiler; Michaelis, E. W.; Meckenstock, R. U. Microbial in situ degradation of aromatic hydrocarbons in a contaminated aquifer monitored by carbon isotope fractionation. *J. Contam. Hydrol.* **2003**, *65*, 101−120.

(6) Schwarzenbach, R. P.; Gschwend, P. M.; Imboden, D. M. *Environmental Organic Chemistry;* Wiley: New York, 1993.

(7) Harrington, R. R.; Poulson, S. R.; Drever, J. I.; Colberg, P. J. S.; Kelly, E. F. Carbon isotope systematics of monoaromatic hydrocarbons: vaporization and adsorption experiments. *Org. Geochem.* **1999**, *30*, 765−775.

(8) Slater, G. F.; Ahad, J. M. E.; Sherwood Lollar, B.; Allen-King, R.; Sleep, B. Carbon Isotope Effects Resulting from Equilibrium Sorption of Dissolved VOCs. *Anal. Chem.* **2000**, *72*, 5669−5672.

(9) Schueth, C.; Taubald, H.; Bolano, N.; Maciejczyk, K. Carbon and hydrogen isotope effects during sorption of organic contaminants on carbonaceous materials. *J. Contam. Hydrol.* **2003**, *64*, 269−281.

(10) Caimi, R. J.; Brenna, J. T. High-precision liquid chromatography−combustion isotope ratio mass spectrometry. *Anal. Chem.* **1993**, *65*, 3497−3500.

(11) Caimi, R. J.; Brenna, J. T. Quantitative evaluation of carbon isotopic fractionation during reversed-phase high-performance liquid chromatography. *J. Chromatogr. A* **1997**, *757*, 307−310.

(12) Anonymous. IAEA-TECHDOC-825; International Atomic Energy Agency: Vienna, 1995.

(13) Slater, G. F.; Dempster, H. S.; Sherwood Lollar, B.; Ahad, J. M. E. Headspace Analysis: A New Application for Isotopic Characterization of Dissolved Organic Contaminants. *Environ. Sci. Technol.* **1999**, *33*, 190−194.

(14) Yang, Y.-H.; Koopal, L. K. Immobilisation of humic acids and binding of nitrophenol to immobilised humics. *Colloids Surf., A* **1999**, *151*, 201−212.

(15) Voskamp, M. Untersuchungen zur Sorption an Huminstoffen: Molekulargewicht und Kohlenstoff-Isotopenfraktionierung. Ph.D. Thesis, University of Leipzig, Germany, 2004.
(16) Katz, E. *Handbook of HPLC*; Chromatographic Science Series 78, Marcel Dekker: New York, 1998.
(17) Poulson, S. R.; Drever, J. I. Stable Isotope (C, Cl, and H) Fractionation during Vaporization of Trichloroethylene. *Environ. Sci. Technol.* **1999**, *33*, 3689−3694.
(18) Leibnitz, E.; Struppe, H. G. *Handbuch der Gaschromatographie*; Geest & Portig: Leipzig, Germany, 1970.
(19) Vieth, A.; Mueller, J.; Strauch, G.; Kaestner, M.; Gehre, M.; Meckenstock, R. U.; Richnow, H. H. *In-situ* biodegradation of tetrachloroethene and trichloroethene in contaminated aquifers monitored by stable isotope fractionation. *Isotopes Environ. Health Stud.* **2003**, *39*, 113−124.
(20) Griebler, Ch.; Safinowski, M.; Vieth, A.; Richnow, H. H.; Meckenstock, R. U. Combined Application of Stable Carbon Isotope Analysis and Specific Metabolites Determination for Assessing In Situ Degradation of Aromatic Hydrocarbons in a Tar Oil-Contaminated Aquifer. *Environ. Sci. Technol.* **2004**, *38*, 617−631.
(21) Goedeke, S.; Weiss, H.; Richnow, H. H.; Borsdorf, H.; Trabitzsch, R.; Dietze, M.; Schirmer, M. Tracertest zur Analyse des reaktiven Transports im Aquifer am Industriestandort Zeitz. *Altlasten Spektrum* **2004**, *13* (4), 1−9.
(22) Chriss, R. E. *Principles of Stable Isotope Distribution*; Oxford University Press: New York, 1999; ch. 3.4, pp 105−116.
(23) Levenspiel, O. *Chemical Reaction Engineering*, 2nd ed.; J. Wiley & Sons: New York, 1972; ch. 10.

Received for review September 13, 2004. Revised manuscript received May 13, 2005. Accepted May 23, 2005.

ES040096N